PNAS RESEARCH ARTICLE | SYSTEMS BIOLOGY

The parasite intraerythrocytic cycle and human circadian cycle are coupled during malaria infection

Francis C. Motta[a,1], Kevin McGoff[b], Robert C. Moseley[c], Chun-Yi Cho[d], Christina M. Kelliher[e], Lauren M. Smith[f], Michael S. Ortiz[g], Adam R. Leman[h], Sophia A. Campione[f], Nicolas Devos[i], Suwanna Chaorattanakawee[j], Nichaphat Uthaimongkol[k], Worachet Kuntawunginn[k], Chadin Thongpiam[k], Chatchadaporn Thamnurak[k], Montri Arsanok[k], Mariusz Wojnarski[l], Pattaraporn Vanchayangkul[k], Nonlawat Boonyalai[k], Philip L. Smith[m], Michele D. Spring[k], Krisada Jongsakul[k], Ilin Chuang[n], John Harer[o], and Steven B. Haase[f,p,1]

Edited by Joseph Takahashi, The University of Texas Southwestern Medical Center, Dallas, TX; received September 27, 2022; accepted May 9, 2023

During infections with the malaria parasites *Plasmodium vivax*, patients exhibit rhythmic fevers every 48 h. These fever cycles correspond with the time the parasites take to traverse the intraerythrocytic cycle (IEC). In other *Plasmodium* species that infect either humans or mice, the IEC is likely guided by a parasite-intrinsic clock [Rijo-Ferreira*et al.*, *Science* **368, 746–753 (2020); Smith *et al.*, *Science* **368**, 754–759 (2020)], suggesting that intrinsic clock mechanisms may be a fundamental feature of malaria parasites. Moreover, because *Plasmodium* cycle times are multiples of 24 h, the IECs may be coordinated with the host circadian clock(s). Such coordination could explain the synchronization of the parasite population in the host and enable alignment of IEC and circadian cycle phases. We utilized an ex vivo culture of whole blood from patients infected with *P. vivax* to examine the dynamics of the host circadian transcriptome and the parasite IEC transcriptome. Transcriptome dynamics revealed that the phases of the host circadian cycle and the parasite IEC are correlated across multiple patients, showing that the cycles are phase coupled. In mouse model systems, host–parasite cycle coupling appears to provide a selective advantage for the parasite. Thus, understanding how host and parasite cycles are coupled in humans could enable antimalarial therapies that disrupt this coupling.**

host–parasite interaction | intraerythrocytic development cycle | circadian rhythm | *plasmodium vivax* | gene expression

Significance

We provide direct evidence that the parasite's intrinsic developmental cycle is aligned to the host's circadian rhythm during malaria infection. This alignment suggests an evolutionary adaptation that creates synchrony between parasites during the blood phase and a method for evading host defenses or optimizing utilization of host resources that are controlled by the host circadian clock. This work opens the door for chronotherapeutic strategies for treating malaria infections.

Malaria disease in humans, caused by infection with the parasite genus *Plasmodium*, remains a global health crisis with an estimated 241 million cases and 627,000 deaths worldwide in 2020 (1). Effective treatment is complicated by the continued development of drug resistance, already established in *Plasmodium falciparum* and emerging in *Plasmodium vivax* (2–4). Drug resistance, combined with the threat of zoonotic jumps to humans by simian-infecting parasites (5), is motivating researchers to better understand fundamental *Plasmodium* biology in the hopes of revealing novel drug targets and innovative and improved methods of treatment (6, 7).

The multistage lifecycle of *Plasmodium* includes a distinct intraerythrocytic developmental cycle (IEC) inside the host organism that is characterized by periodic rupture, egress, and (re)invasion of host erythrocytes (red blood cells, RBCs). While inside an RBC, *Plasmodium* is observed to progress through morphologically distinct stages ending with the schizont stage, during which the parasite undergoes multiple rounds of asexual division. The resulting merozoites then rupture the RBC and rapidly infect new RBCs, beginning the cycle anew.

For human-infecting *Plasmodium* species, the infecting parasite populations synchronously advance through the IEC, maintaining precise periods of 24, 48, or 72 h depending on the species. Recent evidence suggests that the maintenance of synchronized progression through the *Plasmodium* IEC, and thus the synchronized bursting of RBCs and subsequent release of parasites, is controlled by parasite-intrinsic molecular oscillators that may interact with host circadian cycles (8, 9). Like circadian clocks, the parasite clock appears to control large programs of transcriptional dynamics. Because intrinsic clock mechanisms were identified in divergent *Plasmodium* species that infect both mouse and humans, we expect that intrinsic clock mechanisms are likely a fundamental feature of malaria parasites.

Intrinsic clock control of synchronized bursting on its own may provide a benefit to the infecting parasite populations—either by overwhelming the host immune system (10) or through evasion of the immune response (11). Furthermore, alignment of the synchronized IEC to the host circadian rhythm could benefit the parasite by avoiding peaks of some immune activity that may be under circadian control (12, 13), such as rhythmic

Author contributions: F.C.M., K.M., C.-Y.C., C.M.K., A.R.L., N.D., S.C., P.L.S., M.D.S., K.J., I.C., J.H., and S.B.H. designed research; F.C.M., K.M., C.-Y.C., C.M.K., L.M.S., M.S.O., A.R.L., N.D., S.C., N.U., W.K., C. Thongpiam, C. Thamnurak, M.A., M.W., P.V., N.B., M.D.S., K.J., I.C., and S.B.H. performed research; F.C.M., K.M., and S.B.H. contributed new reagents/analytic tools; F.C.M., K.M., R.C.M., C.M.K., L.M.S., S.A.C., I.C., and S.B.H. analyzed data; F.C.M., W.K., C. Thongpiam, and M.A. performed validation; F.C.M., W.K., C. Thongpiam, C. Thamnurak, P.L.S., and K.J. provided resources; F.C.M., R.C.M., S.A.C., and I.C. performed data curation; W.K., P.V., N.B., M.S., P.L.S., I.C., and S.B.H. provided project supervision; M.W., P.L.S., I.C., and S.B.H. performed project administration; J.H. and S.B.H. performed funding acquisition; F.C.M. and R.C.M. created all figures; and F.C.M., R.C.M., M.D.S., and S.B.H. wrote the paper.

The authors declare no competing interest.

This article is a PNAS Direct Submission.

[1]To whom correspondence may be addressed. Email: fmotta@fau.edu or shaase@duke.edu.

This article contains supporting information online at https://www.pnas.org/lookup/suppl/doi:10.1073/pnas.2216522120/-/DCSupplemental.

Published June 6, 2023.

fluctuation of immune cells in blood (14). Alternatively, parasites may time their reproduction to maximize access to host resources (15, 16). This alignment could help explain the apparent reduced parasite fitness induced by misalignment of the IEC stage and mouse host circadian phase (13, 17, 18). However, whether the *Plasmodium* IEC aligns with the host circadian rhythms in humans is unknown.

Does the *Plasmodium* IEC align its intrinsic rhythm with the host circadian rhythms in humans? In this study, we examine the alignment of transcriptional phases of the *P. vivax* IEC to human host circadian rhythm across a cohort of 10 human-parasite pairs. Using high-resolution time series transcriptomics to measure both host circadian and parasite IECs, we observe a significant correlation between the phases of the parasite IEC and the host circadian rhythm. These findings provide evidence that the oscillators controlling the parasite IEC in human-infecting *Plasmodium* parasites are coupled to the host circadian rhythm.

Results

Gene Expression Dynamics of Host and Parasite Cycles in Cultured Whole Blood from Infected Hosts Exhibit Rhythmic Behavior. Both circadian clocks (19) and intrinsic *Plasmodium* oscillators (8, 9) control well-ordered cyclic programs of transcriptome dynamics. To ask whether parasite and host rhythms were aligned, we simultaneously assayed transcriptome dynamics in both host and parasite using time series RNA-seq analysis on the blood of *P. vivax*–infected subjects.

Nineteen adult participants (anonymized as participants 01 to 19) voluntarily presented at clinics in Na Chaluai and Buntharik Districts in Ubon Ratchathani Province, Thailand, seeking treatment for suspected malaria infection. Prior to treatment, each participant underwent screening for study enrollment (see *Materials and Methods* for study design and inclusion criteria details). Following the initial screening, 10 of the 19 participants (participants 02, 08, 09, 10, 11, 13, 16, 17, 18, and 19) were enrolled in part B, and whole blood samples were collected and further divided into 16 samples (Fig. 1*A*). Other participants exhibited insufficient parasitemia levels or did not meet all inclusion criteria. All eligible participants' parasite populations were determined by microscopy to be well synchronized (greater than 80%) in the early trophozoite developmental stage at the time of the screening (Dataset S1 and Fig. 1*B*).

Participants entered the clinics, were screened, and enrolled across a wide range of times of day (Fig. 1*C*). After a delay following collection (Fig. 1*C*), each of the 16 whole blood aliquots was initially processed (*Materials and Methods*) and then frozen roughly every 3 h over 45 h (Fig. 1*D*). All but one sample (timepoint number nine corresponding to hour 24 for participant 18) survived for subsequent RNA sequencing (Fig. 1*D*). Reads from RNA sequencing of the remaining 159 samples were aligned to both human and *P. vivax* transcriptomes, quantified using TPM and QN, and minimally postprocessed (*Materials and Methods*) to produce 10 pairs of 16-timepoint time series datasets capturing ex vivo, whole transcriptome abundance profiles for human participants and their *P. vivax* populations over 45 h. Read mapping percentages reported by the RNA sequencing read alignment are provided in *SI Appenndix*, Fig. S1.

We identified periodic behaviors in the transcriptomes of both the parasite and the host over the time series representing the parasite developmental cycle and the host circadian cycle, respectively (*SI Appendix*, Fig. S2 and Datasets S2 and S3). Focusing on

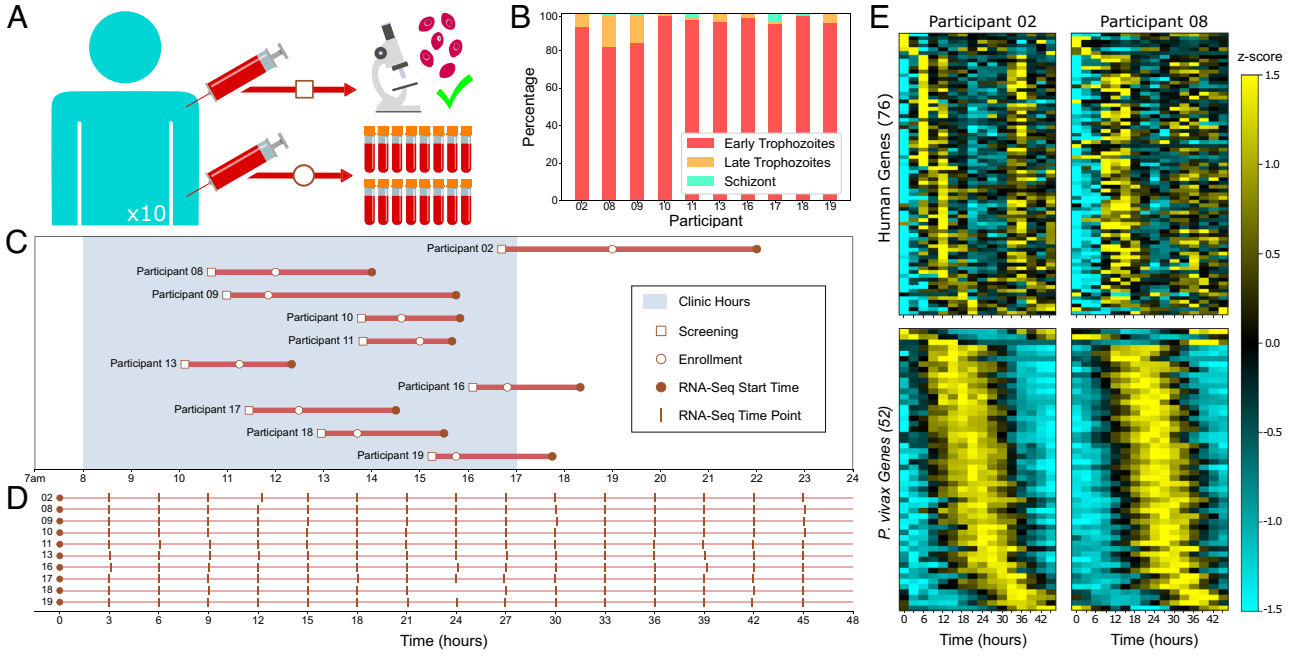

Fig. 1. Experimental protocol and data collection. (*A*) Diagram of the clinical study sampling design. Each participant underwent a single blood draw that is used for screening to ensure uncomplicated monoinfection by *P. vivax*, and a second draw used for RNA sequencing. If the microscopy screening showed asexual parasitemia ≥0.1% and hematocrit ≥25%, and parasites were observed to be well synchronized in the early or late trophozoite phase, the participant was enrolled, and a second blood draw was taken and divided into 16 parts for subsequent RNA-Seq analysis. (*B*) *P. vivax* developmental stage percentages at the screening time for each participant. (*C*) Times of day at which each study participant was screened and enrolled and the times of day of the first timepoints in the RNA-Seq time series experiments. (*D*) For each participant, the times relative to the start time at which each of the 16 samples were aliquoted and frozen for later RNA sequencing. (*E*) Representative z-score heatmaps of genes which exhibit periodic expression patterns at a specified period (24 h for human genes and 48 h for *P. vivax* genes) in participants 02 and 08. For each participant and each organism, periodic genes are taken to be those whose maximum expression across the time series is at least 1 QN TPM and which exhibit at least the same degree of periodicity as the top 5% of genes when ranked by the JTK periodicity score. Genes are consistently ordered in each pair by participant 02's peak expression time during the first period.

rhythmic transcripts that are common to participant pairs, we observed a high degree of similarity in the ordering of peak expression and the dynamics of expression across all pairs of parasite IEC transcriptomes and many pairs of human circadian transcriptomes (Fig. 1*E*, *SI Appendix*, Fig. S3, and Datasets S2 and S3). Also, the periodic transcript programs of parasites and humans appear qualitatively to be largely well aligned. For example, subsets of rhythmic genes common to both participants 02 and 08 appear by eye to be consistently ordered in both the human and the *P. vivax* populations (Fig. 1*E* and Datasets S2 and S3). Moreover, there is a noticeable shift forward in expression peaks of participant 08 compared with 02 in both the parasite sample and the human sample. This suggests that participant 02's host and parasite transcriptional phases were both slightly ahead of participant 08's. These qualitative phase shifts are apparent across many pairs in which heatmaps show enough consistency in gene order to make a qualitative assessment of the relative transcriptional phases by visual inspection (*SI Appendix*, Fig. S3 and Datasets S2 and S3). Analogous figures—with each of the other participants serving as the reference—can be generated using the data and code repositories associated with this manuscript. See Datasets S2 and S3 for the lists of genes and the order they appear in heatmaps presented in this study, as well as time series expression profile statistics for all human and *P. vivax* genes with nonzero expression at some timepoint.

***P. vivax* Gene Expression Dynamics Are Similar to Previous Studies.** The ex vivo time series is an approach to examining both host and parasite rhythms by transcriptomic analysis. To verify that this approach was producing results similar to those observed previously in studies examining only host *or* parasite rhythms, we quantitatively compared our data to earlier studies.

Periodic transcription of temporally ordered genes in the IEC has been confirmed in previous studies across different malaria species (9, 20). Other studies involving *P. vivax* used an ex vivo system in which white blood cells were removed by filtration and utilized a microarray platform for measuring transcriptome dynamics rather than an RNA-Seq platform utilized in this study (20). Thus, these other studies were unable to simultaneously assess both parasite and host rhythms.

First, we compared *P. vivax* transcript dynamics in this study to the dynamics of three *P. vivax* isolates published in ref. 20. While phase-shifted mostly between 3 to 6 h from the *P. vivax* isolates in ref. 20, all ten participants displayed highly similar transcript dynamics to all three isolates (Fig. 2*A*). Temporal ordering of highly periodic genes appears to be conserved between the *P. vivax* parasites in our participants and the *P. vivax* isolates in ref. 20 (Fig. 2*B* and Dataset S3). In both studies, peaks of gene expression are evenly distributed throughout the IEC (Fig. 2*B* and Dataset S3). Also, the beginning of a second wave of gene expression—indicated by the increasing gene expression of early phased IEC genes later in the time series—is clearly visible (Fig. 2*B*). The gene expression of some late IEC phased genes appears at the beginning of the time series in our participants (presumably from the previous cycle) (Fig. 2*B* and Dataset S3). Notably, participant 09 appears phased almost halfway through the IEC cycle ahead of the other nine participants (Fig. 2*A*).

A Circadian Signal Is Detectable in Ex Vivo Whole Blood Samples. Previous studies examining circadian gene expression in human whole blood have found the circadian signal to be weaker than that found in other tissues in which many genes are known to be highly rhythmic (21, 22). We also expect that factors related to ex vivo sampling in our study could contribute to degradation of the circadian signal. For example, our samples were collected ex vivo, and so all environmental entrainment signals (e.g., light/dark cycles and eating) have been removed, which may contribute to a reduced circadian signal as natural variability in oscillation periods will cause synchrony loss across a population or cells (23). Additionally, our study covers two circadian cycles (two 24-h periods), which can further dampen the circadian signal, due in part to synchrony loss. Finally, it is not clear that human peripheral blood mononuclear cells would remain healthy in ex vivo culture, which could certainly affect the circadian rhythm or the integrity and stability of transcripts.

In addition to ex vivo conditions, a variety of lifestyle and environmental variables encountered by participants in this study could impact rhythmicity. Some of the participants are night shift workers, while others reported sleep disruptions (Dataset S1), both known factors that can impact circadian rhythmicity in blood (21, 22). Also, we cannot rule out the impacts, direct or indirect, that malaria infection may have on a person's circadian rhythm.

To estimate the cumulative effect of the above issues on the detection of circadian rhythmicity, we compared our participants' circadian transcriptomes to a controlled study that investigated the impacts of sleep deprivation on the circadian transcriptome in human whole blood (21). We found only a moderate decrease in the percentage of circadian transcripts found in our participants compared to participants under normal sleep conditions (Fig. 2*C*). This moderate decrease in circadian signal in our participants compared to in vivo data under normal sleep conditions is comparable to those seen in participants with sleep-deprived conditions compared to normal sleep conditions. In particular, the median percentage of rhythmic genes in the in vivo sleep study under sleep deprivation conditions dropped by between 0.46% and 1.82% across the range of thresholds, while our ex vivo study observed the percentage of rhythmic genes drop by between 0.4% to 2.24% across the same thresholds (Fig. 2*C*). In aggregate, approximately 60% of the rhythmic (JTK *P* value threshold below 0.1) genes in the 10 participants in the present ex vivo study were also rhythmic in at least one of the 14 participants in the in vivo sleep study (*SI Appendix*, Fig. S4). Despite the relatively high number of total transcripts meeting this JTK *P* value threshold in all conditions, we found high variability in the identities of the periodic genes across participants (Fig. 2*D*). To investigate whether the rather limited overlap of cycling genes between participants was expected, or was a result of factors particular to this study, we asked whether a similar observation held for pairs of participants in the in vivo sleep deprivation study (21). We found that the median percentage of common rhythmic genes out of the combined rhythmic genes among pairs of participants during the baseline normal sleep conditions in the in vivo study was only 1.07% at the strict JTK *P* value threshold of 0.05. Under sleep deprivation conditions, this percent overlap dropped to 0.87%, compared to a 0.61% overlap observed among the ten participants in this ex vivo study (Fig. 2*D*). These percent overlaps increased to only 2.05%, 1.50%, and 1.13%, respectively, in the in vivo baseline condition, in vivo sleep deprivation, and ex vivo condition at the more relaxed JTK *P* value threshold of 0.1 (Fig. 2*D*). These comparative results suggest that a circadian signal observed in the whole blood of the ten participants in this study remains detectable ex vivo but may be partially degraded by a combination of internal and external factors.

***P. vivax* IEC Phase and Host Circadian Phase Are Correlated.** Recent studies demonstrate that an intrinsic clock controls the IEC of some malaria parasite species (8, 9). In studies involving mice-infecting *Plasmodium* species with 24-h IECs, their cycles

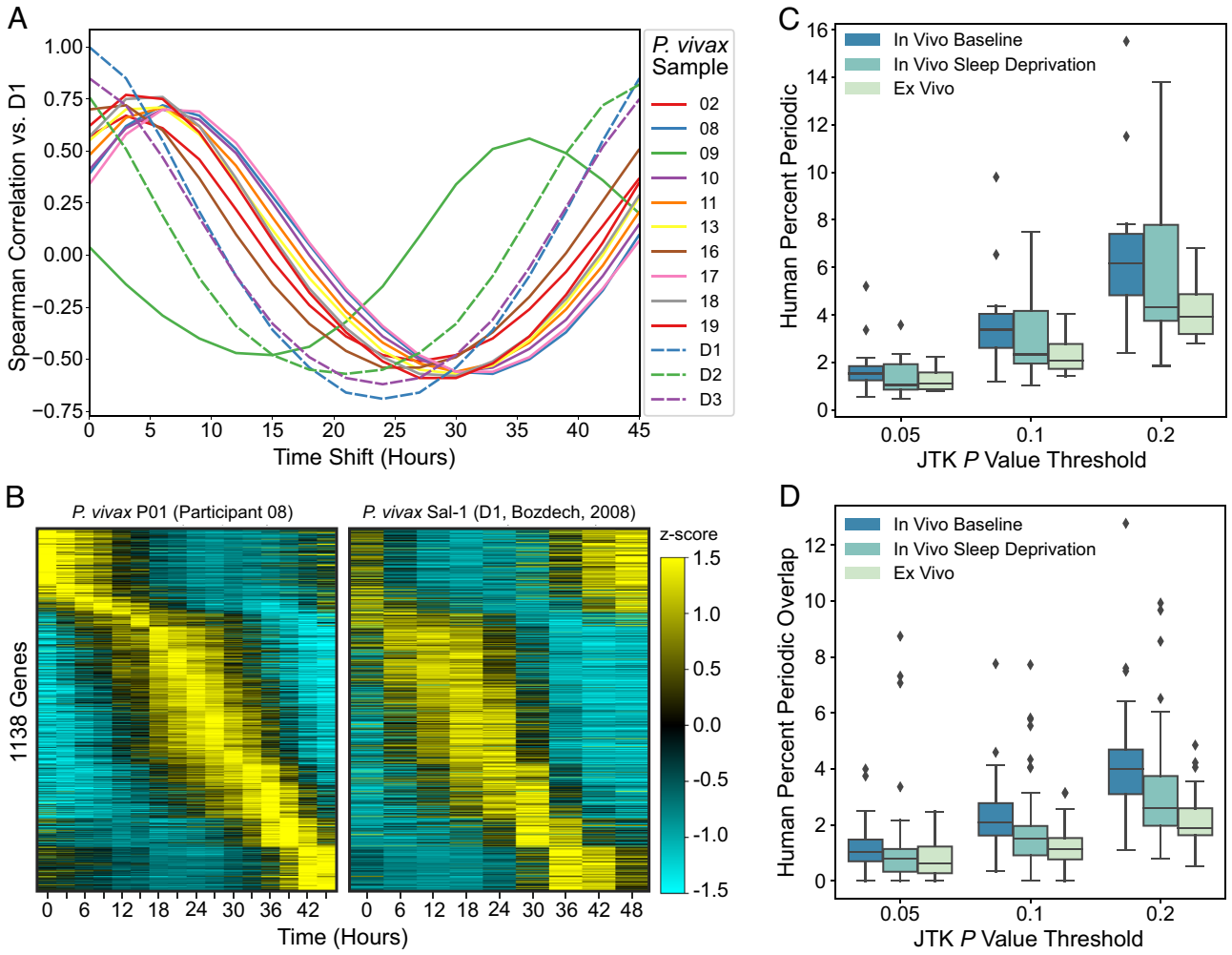

Fig. 2. Comparisons of RNA-Seq time series data to earlier studies. (*A*) The average pairwise Spearman correlation between one of the *P. vivax* (Sal-1) isolates from the ex vivo time series RNA-Seq experiment reported in ref. 20, the other two samples reported in that study, and each of the 10 participants in this study. Correlations are the average over all timepoints shifted by the specified amount, with wrapping assuming a 48-h period. (*B*) z-score heatmaps of highly periodic (JTK *P* value ≤ 0.005) *P. vivax* (P01) genes in participant 08 that also appear in sample D1 from ref. 20. All heatmaps contain 1,138 genes and are ordered by the time of peak expression in participant 08. Analogous plots can be generated for the other participants using data and code repositories associated with this manuscript (*SI Appendix*, Table S3). (*C*) Box-and-whisker plots comparing the average percentage of expressed genes common to the three conditions and achieving the specified JTK *P* value thresholds. (*D*) Box-and-whisker plots comparing the average percent overlap among the rhythmic genes achieving the specified JTK *P* value thresholds. Distributions in *C* represent either the 14 participants in the in vivo study (21), under baseline or sleep deprivation conditions, or the 10 participants in this study. Distributions in *D* represent all participant pairs within each study. In *C* and *D*, boxes indicate distribution quartiles, and whiskers extend from minimum sample values to samples at most 1.5 times the interquartile ranges, with values outside this range plotted as outliers.

appeared to be well aligned with the 24-h circadian cycle of the host (8, 17) and that alignment of parasite and host cycles was observed to be important to maintain parasite fitness. Here, we aimed to determine whether a similar alignment of the *P. vivax* 48-h IEC could be observed with the host circadian clock in humans.

By visual inspection, the apparent timings of peak expression in rhythmic *P. vivax* genes show notable qualitative shifts between pairs of participants (*SI Appendix*, Fig. S5*A* and Dataset S3). The largest phase shifts between any pair of participants occurs between 09 and all other participants, which is consistent with the peak correlation shown in Fig. 2*A*, refined microscopy staging data (*SI Appendix*, Figs. S5*B* and S6) and physiological indicators (*SI Appendix*, Fig. S5*C*). For a detailed discussion of participant 09, see the Supporting Text in *SI Appendix*. We asked whether the phase shifts in *P. vivax* IEC rhythms between all participants correlated with the observed shifts in the host circadian rhythms. To address this question, we developed a data-driven pipeline to estimate the relative circadian transcriptional phase shifts between human participants and, separately, the relative IEC transcriptional phase shifts between their infecting parasites (*Materials and Methods*).

If a *P. vivax* parasite, with its 48-h IEC, has aligned a particular phase of its cycle (e.g., the egress from host RBCs) to a particular circadian phase in the host, with a 24-h circadian cycle, then there would be a constant phase difference between the circadian phase of the host and twice the parasite IEC phase, as illustrated in Fig. 3*A*. Since *P. vivax's* expected IEC period length is twice as long as a host's expected circadian period, the time rate of change of the circadian phase should be twice the rate of change of the IEC phase. Therefore, if there is a parasite–host phase alignment, then the circadian phase difference between two hosts would be well correlated with twice the IEC phase difference between their parasite populations.

To estimate the transcriptional circadian phase difference between each pair of human participants, and separately the transcriptional IEC phase between their parasite populations, we computed the circular mean phase difference between subsets of human and *P. vivax* genes that were most highly expressed and most highly oscillatory (at 24 and 48 h, respectively) in both samples (Fig. 3*B* and *SI Appendix*, Fig. S7 *A* and *B*). Specifically, within each species and for each participant, genes which exhibit

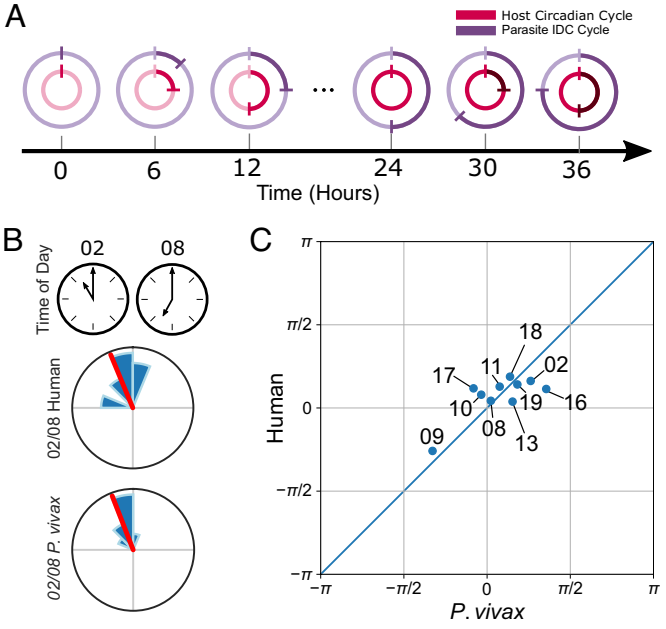

Fig. 3. Human phase, *P. vivax* phase, and wall time circular correlations. (*A*) Cartoon illustrating the correspondences between elapsed time and the phases of a 48-h cycle and a 24-h cycle, indicating that the difference between the circadian cycle phase and twice the intraerythrocytic developmental cycle phase is expected to be constant over time. (*B*) The times of day on 24-h clocks of the first timepoints in the RNA-Seq time series (*Top*) and the histograms of gene phase differences estimated from the overlapping periodic human (*Middle*) and *P. vivax* (*Bottom*) genes for participants 02 and 08. The radii of the histogram slices have been scaled so the area of each slice is proportional to the number of data points it represents. (*C*) Scatter plots of inferred human and *P. vivax* phases. For *P. vivax*, all phase difference estimates were first multiplied by two and reduced modulo 2π before visualization. All phases are shifted to the interval $[-\pi, \pi)$ radians, and the 0 phases were chosen to be the circular-mean human phase. The left and right edges and the top and bottom edges should be identified since the phase/angle $-\pi$ is equal to π on a circle.

at least 10 QN TPM during the time course were identified, and the top 3% of these genes by their JTK periodicity score were retained. This resulted in an average of 219.9 (57.5 IQR) human and 207.9 (14.5 IQR) *P. vivax* genes across the 10 participants and an average of 7.9 (5) human and 45.1 (37) *P. vivax* genes across the pairwise intersections (Table 1). For all pairwise intersection sizes, see the UpSet plots in *SI Appendix*, Figs. S8 and S9, and for complete lists of periodic gene identities and expression profiles meeting these (and other) expression and periodicity thresholds, see the tables in Datasets S4–S19. From the genes in the pairwise intersections, 45 pairwise circadian phase difference estimates for human samples and 45 pairwise IEC phase difference estimates for *P. vivax* samples were computed. Fig. 3*B* and *SI Appendix*, Fig. S7 *A* and *B* shows phase difference histograms over rhythmic genes that are common to a participant pair. We observe that the distributions of phase shifts of the parasite genes are very tightly distributed, while there is larger variance in the circular distributions of phase shifts of the human genes (Table 1). Note that the mean phase shift of the human genes reinforces the qualitative observation that 02 is phase advanced relative to 08, as does the mean phase shift of the parasite genes (Fig. 3*B*).

The inferred phase differences between participants need not be entirely consistent with one another. For example, the pairwise phase difference between samples A and C need not be equal to the sum of the differences between A and B and B and C, as would necessarily be the case if phases were assigned directly to each A, B, and C. Such inconsistencies may be due to different numbers and identities of periodic genes in each pairwise intersection. It is expected that some pairwise phase difference estimates will be less reliable than others (*SI Appendix*, Fig. S7*C*).

To correct errors in the pairwise phase estimates and compute a single circadian phase estimate for each human sample and a single IEC phase estimate for each *P. vivax* sample, we independently applied a phase synchronization method (24) to each collection of 45 pairwise phase estimates in hosts or parasites. Briefly, phase synchronization determines a globally consistent choice of phase variables that best explain a collection of noisy pairwise phase differences. Unlike the pairwise circadian phase estimates, the *P. vivax* pairwise phase estimates were already remarkably globally concordant, exhibiting a high confidence circular correlation of 0.996461 (*P* value: 0.000004) with the pairwise phase difference estimates computed after phase synchronization (*SI Appendix*, Fig. S7*C*).

Importantly, our method of computing sample phase differences is entirely data driven and depends on limited assumptions. For example, it makes no assumptions about particular transcripts that will reflect a circadian phase in whole blood during malaria infection, and instead, it only assumes that the relative transcriptional phases in each organism will be most reliably estimated by subsets of highly expressed genes oscillating with the correct period. Moreover, this process uses multiple subsets of overlapping gene sets to derive globally consistent estimates of phases that best explain the pairwise phase differences seen in the data, some of which will undoubtedly be less reliable than others.

To compare the relative phase differences and identify the degree of alignment between the host circadian and parasite IEC phases, we computed the circular correlation [(25), *Materials and Methods*] of the 10 pairs of estimated phases and found a circular correlation of 0.70 (*P* value: 0.019). The significance of the correlation was computed using an exhaustive permutation test (*SI Appendix*, Fig. S7*D* and Materials and Methods). The circular correlation between two random circular variables is 1.0 if and only if they differ by a constant, and it is invariant under a constant phase shift of either sample. The circadian and IEC phase pairs are plotted in Fig. 3*C*, in which proximity to the diagonal indicates the degree of agreement between the relative phases of the hosts and their parasites. The significant shift in participant 09's estimated IEC phase relative to the other parasite populations agrees with the by-eye estimate of 09's relative phase advance based on the heatmaps shown in *SI Appendix*, Fig. S5*A* (Dataset S3) and the timepoint-wise correlation analysis shown in Fig. 2*A*. To see this, observe that 18 h in a 48-h cycle is $6\pi/8$ radians, which when multiplied by two yields a relative advance of $3\pi/2$ radians, which is equivalent to a relative delay of $-\pi/2$ radians between 09 and the other participants, as seen in Fig. 3*C*. Notably, twice the inferred 09 *P. vivax* phase is in excellent agreement with the inferred 09 human phase (Fig. 3*C*). Given an alignment between the *P. vivax* IEC phase and the host circadian phase, there necessarily will be two IEC phases corresponding to each host phase, (e.g., timepoint 0 and timepoint 24 in Fig. 3*A*). Thus, it is not surprising that among hosts with similar circadian phases, we observe a parasite population which has progressed roughly halfway through its IEC cycle relative to the other parasites. In this way, participant 09 is not an outlier, but rather confirms expectation.

The correlation between the estimated circadian phases and the time of day of the first timepoint in the RNA-Seq time series was found to be only 0.31 (*P* value: 0.178). To try and control for any underlying differences in the circadian phases of participants, we additionally computed correlations between circadian transcriptional phases and the phases determined by the times between each participant's first RNA-Seq measurement and their

Table 1. Periodic gene statistics

Threshold		Periodic gene counts		Gene intersection counts		Phase shift variance	
Expression	Periodicity (human, *P. vivax*), %	Human	*P. vivax*	Human	*P. vivax*	Human	*P. vivax*
10	(1, 3)	74.7 (14.75)	207.9 (14.5)	0.95 (1)	45.1 (37)	1.6e-02 (1.4e-02)	1.6e-03 (1.3e-03)
	(3, 3)	219.9 (57.5)		7.9 (5)		2.4e-02 (3.3e-02)	
	(5,5)	344.9 (68.75)	324.3 (34.5)	17.3 (9)	89.5 (55)	3.3e-02 (2.4e-02)	1.9e-03 (1.9e-03)
	(10, 5)	736.2 (263.5)		68.8 (28)		4.0e-02 (2.1e-02)	
5	(3, 3)	325.2 (66.25)	221.4 (10.25)	11.6 (6)	49.1 (27)	3.1e-02 (2.6e-02)	1.6e-03 (1.3e-03)
	(5,5)	553.5 (65.75)	335.7 (32.5)	30.6 (13)	93.2 (54)	3.7e-02 (2.1e-02)	1.8e-03 (1.8e-03)
	(10, 5)	1,036.0 (105.0)		104.2 (37)		4.3e-02 (2.7e-02)	
1	(3, 3)	583.3 (127.0)	223.7 (12.75)	22.2 (11)	49.5 (27)	3.7e-02 (2.6e-02)	1.7e-03 (1.6e-03)
	(5,5)	982.8 (201.75)	339.5 (30.75)	56.9 (27)	94.1 (53)	4.1e-02 (2.4e-02)	1.9e-03 (1.9e-03)
	(10, 5)	1,933.7 (796.0)		207.8 (77)		4.6e-02 (2.8e-02)	

The average counts of periodic genes across participants, the average counts of the pairwise intersections across all participant pairs, and the average circular variances of pairwise phase shift estimates of periodic genes across all participant pairs with two or more overlapping genes. Interquartile ranges are given in parentheses. Periodic genes are taken to be those whose maximum expression across the time series is at least the specified expression threshold in QN TPMs and which exhibit at least the same degree of periodicity as the top X of these genes when ranked by the JTK periodicity scores. Pairs of periodicity thresholds specify those used for humans and *P. vivax* samples.

self-reported usual to-sleep and wake-up times as well as their self-reported recent sleep and wake times (Dataset S1) and found the correlation somewhat improved for the recent sleep-adjusted wall times to 0.44 (*P* value: 0.102) (Table 2) but remained below the host–parasite correlation.

Threshold restrictions on expression level and periodicity score could yield too few genes in the pairwise intersections of human samples to provide reliable estimates of circadian phases—as noted earlier, we observed high variability of the rhythmic human genes across participants (*SI Appendix*, Fig. S8). To assess the sensitivity of our conclusions to the choice of periodicity and activity thresholds, we considered a wide range of thresholds, dramatically relaxing them in humans, thereby increasing the numbers of genes considered to be periodic, and increasing the average numbers of genes in the pairwise intersections between participants up to several hundred (Table 1, *SI Appendix*, Figs. S8 and S9, and Datasets S5–S19). We found that the conclusions are qualitatively insensitive, with high correlations [0.57 (*P* value: 0.054) to 0.71 (*P* value: 0.023)] between host and parasite phases exhibited across the tested ranges of periodicity and activity thresholds (Table 2). On the other hand, a periodicity threshold that is too permissive could include genes with unreliable phase estimates. Thus, we additionally tightened the human periodicity threshold and computed circular correlations implied by the top 1% most periodic human genes meeting the 10 TPM expression filter. In this case, only 21/45 pairwise intersections contained any genes, and many pairwise phase differences were estimated by the phase calls of a single gene (*SI Appendix*, Fig. S8 and Dataset S4). Still, this limited but highly periodic gene set implied a significant correlation between the host and parasite phases [0.56 (*P* value: 0.048), Table 2)].

Discussion

This study demonstrates evidence that the transcriptional phase of the *P. vivax* parasite population during the IEC is well aligned with the circadian transcriptional phase of its human host. This study does not address any mechanism(s) that may be driving the synchronization of individual parasites within the population, or the alignment with the host, although several theories have been put forward in other systems (16, 26, 27).

This study affirms that *P. vivax* patients can present with 80% trophozoites throughout the day (Fig. 1*C* and Dataset S1) and explains why clinicians should not expect to see fevers spiking at the same time every day in their malaria patients. However, the clinics in which volunteers were enrolled did not operate 24 h per

Table 2. Phase circular correlations

Threshold		Phase circular correlation					
Expression	Periodicity (human, *P. vivax*), %	*P. vivax*	Wall time	Adjusted by recent sleep	Adjusted by recent wake	Adjusted by usual sleep	Adjusted by usual wake
10	(1, 3)	0.56 (0.048)	0.45 (0.09)	0.41 (0.119)	0.24 (0.249)	0.27 (0.229)	0.156 (0.336)
	(3, 3)	0.70 (0.019)	0.31 (0.178)	0.44 (0.102)	0.16 (0.338)	0.22 (0.235)	0.23 (0.298)
	(5, 5)	0.66 (0.037)	0.20 (0.291)	0.33 (0.160)	0.06 (0.430)	0.18 (0.276)	0.18 (0.362)
	(10, 5)	0.71 (0.022)	0.02 (0.553)	0.11 (0.337)	−0.11 (0.594)	−0.09 (0.630)	0.01 (0.608)
5	(3, 3)	0.59 (0.053)	0.15 (0.355)	0.35 (0.148)	0.04 (0.449)	0.10 (0.363)	0.14 (0.407)
	(5, 5)	0.65 (0.039)	0.08 (0.450)	0.21 (0.252)	−0.10 (0.574)	0.01 (0.471)	0.03 (0.562)
	(10, 5)	0.63 (0.062)	−0.07 (0.648)	0.05 (0.447)	−0.16 (0.638)	−0.15 (0.738)	−0.10 (0.673)
1	(3, 3)	0.57 (0.054)	0.18 (0.322)	0.33 (0.176)	−0.12 (0.612)	0.08 (0.416)	−0.01 (0.526)
	(5, 5)	0.60 (0.048)	−0.02 (0.553)	0.08 (0.410)	−0.23 (0.718)	−0.12 (0.659)	−0.15 (0.666)
	(10, 5)	0.62 (0.043)	0.01 (0.517)	0.11 (0.376)	−0.14 (0.621)	−0.06 (0.587)	−0.08 (0.623)

The circular correlations between human circadian phases and either *P. vivax* phases, wall times or sleep/wake-adjusted wall times. Empirical *P* values are given in parentheses. Periodic genes are taken to be those whose maximum expression across the time series is at least the specified expression threshold in QN TPMs and which exhibit at least the same degree of periodicity as the top X% of these genes when ranked by the JTK periodicity scores. Pairs of periodicity thresholds specify those used for humans and *P. vivax* samples.

day, and study B participants were required to have parasite populations in a specific IEC stage. The combination of these two constraints could, in principle, bias the alignment between host and parasite phases, but only if there were very tight coupling between both the coarse IEC stage and the IEC transcriptional phase, and separately the human transcriptional phase and the time of day. This concern is ameliorated by the fact that no participant was rejected due to their parasites being in the wrong stage and because participant 09's parasites indicate that the IEC stage inclusion criteria were not highly restrictive to the range of allowable parasite transcriptional phases. Moreover, we observe a rather low correlation between the host phase and the time of day, which further diminishes concern about any spurious correlation between the hosts and their parasites caused by study constraints.

The rather weak observed circular correlation between the participants' circadian phases and the time of day may have several explanations. Importantly, there exists substantial interindividual variability in the physiological and behavioral manifestations of the circadian system (28, 29), with the distribution of the so-called chronotypes in human populations exhibiting a wide spread—up to 6 h according to some studies (30, 31). In addition to light as an entrainment signal, behavioral factors that could not be entirely controlled for, such as sleep/wake times, feeding times, and exercise are also external cues that can variably influence internal phasing of parts of the circadian system (32). Moreover, the rate and degree of circadian phase adjustment to disruptions or misalignments between behavioral cues and the time of day, as seen in shift workers for example, is highly variable (33). Multiple subjects in the study reported working at night. Finally, we cannot confirm nor rule out the possibility that the parasite populations, through some yet unknown mechanism, are actively perturbing the phase of the host clock to match its IEC phase, as has been seen in other systems (8, 34).

Across the entire volunteer cohort, we observe a significant correlation between the parasite IEC phases and host circadian phases. However, not all participants show the same degree of alignment. One possible explanation is that coupling between the host and the parasite population is a transient phenomenon that requires some amount of time (following egress from the liver and initialization of the IEC) to become established. From a dynamical systems perspective, this is a plausible explanation if the alignment of phases has not already been established during the liver stage since the entrainment of coupled oscillators is known to be a transient phenomenon in many biological systems and their models (35, 36). Interestingly, participant 16, who exhibits one of the largest disparities between host and parasite phases, had no gametocytes present in their parasite population by blood smear microscopy and reported their fever start date on the same day they entered the clinic and the study (Dataset S1). These observations are consistent with a very recent entry into the IEC and the observation that the concentration of parasites that produce gametocytes increases over the course of infection (37). Note that participant 09 also did not show any gametocytemia.

There are multiple limitations of this study. For one, the cohort of participants is small, making it difficult to control for a variety of potentially confounding factors such as age, prior infection, and days since initial infection. Also, transcriptional determinants of IEC and circadian phases from ex vivo whole blood measurements are neither known nor expected to be identical for all individuals. Our data-driven solution requires choices of thresholds to define gene lists, and although the conclusions have been shown to hold over a wide range of thresholds, the circadian signals may be corrupted to some extent by the inclusion of irrelevant genes and/or degraded by the omission of relevant genes. We speculate that degradation of the circadian signal could be further exacerbated by the choice to only compute 24-h periodicity scores of each transcript profile, which is justified by the constraints on the temporal resolution of the RNA-Seq time series and the fact that the free-running circadian periods are known to be highly concentrated around 24 h across individuals (study participants in ref. 38 exhibited a range between 23.56 to 24.70 h), unlike circadian phasing that shows greater variance. Finally, we cannot rule out the possibility that some other choices of expression or periodicity thresholds, a different method of determining what constitutes experimental noise, or some other quantification and ranking of transcript periodicity would yield different conclusions.

The dataset analyzed in this study represents a rich collection of dynamic gene expression data and participant metadata, the depths of which we have only started to explore. Differential expression analysis may enable comparisons between participants and provide hypotheses for correlates with metadata variates. A detailed study of the expression dynamics of participant 09 before and after apparent parasite egress may help distinguish between potential core oscillator components that may be part of an intrinsic oscillator driving rhythmic gene expression and those which may be driven by external cues not present ex vivo. Excitingly, gene regulatory network inference tools may be able to elucidate interactions between host molecular circadian cues and parasite IEC to suggest mechanisms of population synchrony and/or parasite–host phase alignment.

Our finding that the parasite IEC appears to be aligned to the host circadian cycle raises important questions. First, what is the selective advantage of this alignment? Although there is evidence for increased parasite fitness when parasite IEC and host circadian cycles are aligned in mouse systems (17), the mechanism of the advantage is not yet well established. We expect that parasite fitness is also aided in human systems.

A second critical question is by what mechanism is the intrinsic oscillator of the parasite and the circadian clock of the host coupled? One possibility is that there are chemical or physiological signals that can be read by either or both the host and pathogen that enable them to phase align. While it is tempting to speculate that the parasite oscillator is simply entraining to host signals, it is also possible that the parasite is perturbing the host circadian clock to achieve phase alignment.

It has been suggested by studies involving the mouse-infecting *P. chabaudi* parasite that host eating schedules may serve as a mechanism of parasite population synchronization and developmental stage timing (15, 16, 39–41). For example, ref. 15 concludes that parasite proliferation occurs during host food intake and (16) suggests that food intake controls the timing of parasite differentiation and schizogony. Finally, by studying malaria synchrony in mouse mutants with disrupted circadian oscillators, ref. 39 concludes that malaria parasite replication is most likely coordinated to nutrient availability, and not coordinated to the core clock proteins Per1 and Per2. However, recent findings in a mouse system suggest that host circadian clock components may be more important than feeding time for parasite synchrony (8).

We cannot confirm nor rule out the role of eating as a population synchronizer or as a phase entrainment signal for *P. vivax* in humans. Because the conclusions of this study are based on transcription dynamics in whole blood, we cannot distinguish between the roles played by circadian signals in the blood within the ex vivo culture or other physiological signals that entrained the parasite cycle before blood was drawn. Although Per1 and Per2 are core clock components in many mammalian tissues, and have been seen to exhibit 24-h transcriptional rhythmicity in human

peripheral blood mononuclear cells (42), they are not seen to be robustly rhythmic in transcriptional profiling of whole blood samples. Moreover, other circadian signals, including nontranscriptional 24-h oscillations such as peroxiredoxins redox cycles (43), are also present in human blood and may influence the transcriptional circadian signal we observe in our whole blood samples. While the peroxiredoxin cycle in humans does not appear to influence the rhythmicity of the malaria IEC (9), it is possible that it could influence the phasing of the IEC in whole blood samples.

The discovery of the molecular signals that coordinate the phases of the *P. vivax* IEC and the host circadian rhythm will likely have important implications for new antimalarial therapies. If this coordination between parasite and host rhythms increases the fitness of the parasite in humans as it does in mouse systems, then disruption of these signals could reduce parasite fitness and potentially reduce the severity of disease.

Materials and Methods

Further *Materials and Methods* details can be found in *SI Appendix*.

Study Design. This was a minimal risk study enrolling Thai adults diagnosed with P. vivax by rapid diagnostic test or microscopy at various medical facilities in Na Chaluai and Buntharik Districts in Ubon Ratchathani Province, Thailand, between September and November 2016. Those meeting initial inclusion criteria (age >18 y) and exclusion criteria (no signs/symptoms of severe malaria, no antimalarial use in the past 4 wk and not pregnant), underwent venipuncture for peripheral blood smear and complete blood count (CBC). Smears were read by two trained microscopists to verify parasite species, determine the intraerythrocyte development cycle (IEC) stage (e.g., percentage early and late trophozoites and schizonts), and, using CBC results, quantify asexual and sexual parasitemia. Participant details such as age and sex are available in the attached metadata (Dataset S1). All subjects provided written informed consent, and the study protocol was approved by the Walter Reed Army Institute of Research Institutional Review Board (IRB #00000794), the Ethical Committee for Human Subject Research Ministry of Public Health, Thailand (IRB #00001629), and the Duke University Institutional Review Board (IRB #00000125).

Sample Processing and Lab Procedures. Giemsa-stained thick and thin blood smears were prepared, and asexual and sexual parasitemia were independently determined by two microscopists using parasite counts per 200 white blood cells (thick smear) or per 5,000 RBCs (thin smear). Discordant readings were read by a third blinded microscopist and triggered if there was a difference between reader A and B in species, in category assignment for part A, and for difference greater than 50% for part A high parasitemia group (>0.19%) or for part B. The percentage of the parasites in each IEC stage (early and late trophozoites and schizonts) was determined from total parasite asexual counts obtained during readings.

Real-Time PCR Detection of Malaria. The whole blood samples (0.2 mL) collected from part B participants and stored in EDTA tubes were kept frozen at −80 °C. Parasite DNA was extracted using the EZ1 DNA blood kit with an automated EZ1 Advanced XL purification system (Qiagen, Hilden, Germany) to determine the infecting *Plasmodium* species. All participants were determined to have *P. vivax* monoinfection. PCR primers and probes are listed in *SI Appendix*, Table S1.

RNA Isolation and Sequencing. Frozen cell pellets were used for RNA extraction using the Agencourt RNAdvance Blood RNA purification kit and associated protocols. Samples were cleaned before sequencing with the Zymo Research OneStep™ PCR Inhibitor Removal Kit. Isolated RNA was sequenced at the Sequencing and Genomic Technologies Share Resource at Duke University. Libraries were constructed using a kit specific for blood that depleted both ribosomal and globin RNAs. Sequencing was performed on an Illumina HiSeq 4000.

Quantitating RNA Sequencing Data. Each participant's set of Fastq files were aligned to human and parasite genome reference files using STAR (version 2.7.5c) (44) and quantified using RSEM (version 1.3.3) (45). STAR and RSEM indices were first built using the Gencode v36 reference (reference sequence file GRCh38.primary_assembly.genome.fa and annotation file gencode.v36.primary_assembly.annotation.gtf) for human genome alignment and the PlasmoDB v50 (reference sequence file PlasmoDB-50_PvivaxP01_Genome.fasta and annotation file, PlasmoDB-50_PvivaxP01.gff–which was first converted to a .gtf file using the new code scripts created for this study (*SI Appendix*, Table S3)–for parasite genome alignment. For exact STAR commands used, see *SI Appendix* and code repositories associated with this manuscript.

Removal of Unexpressed Genes. Genes which appear in the comprehensive gene annotation file but which were not expressed (i.e., 0 TPM units) at any timepoint by a participant or parasite population were removed.

Removal of Duplicated Pseudoautosomal Genes. Within the GENCODE comprehensive gene annotation file used for this study are 44 genes with duplicate copies in the pseudoautosomal regions on the X and Y chromosomes (*SI Appendix*, Table S2). Since each of these 44 pairs contained two copies of the same gene, quantification resulted in 44 pairs of duplicated expression profiles for each study participant. Because each participant is male, we added together the duplicate expression profiles in the 44 pairs and retained only a single copy of the duplicated genes. In this way, we ensured that pseudoautosomal genes could not have an outsized influence in downstream analyses (e.g., circadian phase estimates) if these genes were found to be highly periodic and sufficiently highly expressed.

Quantile Normalization. Species-specific quantile normalization (QN) was independently applied to each participant's samples and each participant's parasite samples. For details on the QN procedure, see *SI Appendix*.

Interpolation of Time Series Expression Data. Participant 18's h-24 timepoint sample was accidentally destroyed prior to RNA sequencing. Expression levels for this timepoint were interpolated following QN using Piecewise Cubic Hermite Interpolating Polynomial (PCHIP) interpolation (46). PCHIP interpolation was also used to upsample the *P. vivax* microarray expression time series reported in ref. 20 from 6-h sampling to 3-h sampling prior to the timepoint correlation analysis presented in Fig. 2A. Missing timepoints in ref. 21 were also interpolated using PCHIP.

Transcript Periodicity and Phase Estimation. The phase and periodicity of each transcript at a specified period were quantified using the periodicity detection algorithm, JTK-CYCLE (JTK) (47). For all human and *P. vivax* samples, including those from earlier studies, periods were fixed at 24 or 48 h, respectively. Each transcript was also assigned the corresponding minimal Bonferroni-adjusted *P* value which was used throughout to quantify each transcript's periodicity at the specified period. Only transcripts whose QN abundance level exceeded a specified threshold of activity at a minimum of one point during the time series were retained for further analyses, even if a transcript was highly oscillatory according to JTK. Ranges of periodicity and activity thresholds were analyzed to ensure that results were insensitive to these choices (Tables 1 and 2).

Circadian and IEC Phase Estimation. To estimate the transcriptional circadian phase, θ_k, of each participant and the transcriptional IEC phase, ϕ_k, of each parasite sample ($k = 1, \ldots, 10$), we first identified transcripts that exceeded specified periodicity and activity thresholds for each of the 10 human samples and separately for each of the 10 *P. vivax* samples. The 45 pairwise intersections of the human transcript lists, and separately the *P. vivax* lists, were computed to determine the most oscillatory and most highly expressed human or *P. vivax* transcripts common to that pair. The circular difference between the JTK phase estimates was computed for each transcript in each of the pairwise intersections, and the sample circular mean (48) was computed for each pair of samples, separately for humans and parasites. The eigenvector method for solving the angular (phase) synchronization problem (24) was used to compute globally consistent transcriptional circadian phases (up to rotation by a constant) for each of the 10 human samples. Likewise, using the pairwise IEC phase difference estimates, we computed globally consistent estimates of the transcriptional IEC phases for each of the 10 *P. vivax* samples.

Circadian, IEC, and Wall Phase Correlation Analysis. To quantify the degree of correlation between the estimated circadian and IEC phases, the sample circular correlations (25) between $\widehat{\theta} = \left[\widehat{\theta}_1, \ldots, \widehat{\theta}_{10}\right]$ and $2\widehat{\phi} = \left[2\widehat{\phi}_1, \ldots, 2\widehat{\phi}_{10}\right]$ were computed, where $\widehat{\theta}_k$ and $\widehat{\phi}_k$ are, respectively, the circadian phase and IEC phase estimates of participant k. The circular correlation between the estimated transcriptional circadian phases and the wall-time phases was also computed. We

further computed circular correlations between the circadian phases and the circular differences between each participant's time series start time and their self-reported usual wake times. Finally, we computed correlations between the circadian phases and the circular differences between each participant's self-reported recent wake time by adjusting the usual wake time by the self-reported recent changes in sleep habits (Table 2 and Dataset S1). To measure the significance of the sample circular correlations, we computed empirical *P* values through exhaustive permutations of the estimated transcriptional circadian phases.

Data, Materials, and Software Availability. RNA-Seq data; original code and processed data have been deposited in Gene Expression Omnibus and GitLab (GSE209877 (49); https://gitlab.com/biochron/2023-human-vivax-coupling) (50). Previously published data were used for this work. 1. Supporting information datafiles SD1.xls, SD2.xls, and SD3.xls, reported in ref. 20, 10.1073/pnas.0807404105. 2. Datafiles reported in ref. 21, GSE56931.

ACKNOWLEDGMENTS. F.C.M., J.H., and S.B.H. were funded by the Defense Advanced Research Projects Agency, D12AP00025. S.B.H. was also funded by NIH grant R01 GM126555-0. K.M. gratefully acknowledges funding from the NSF grant DMS 1847144. We would also like to thank the laboratory and clinical staff at AFRIMS who assisted with execution of the clinical trial (in alphabetical order): Chaiyaporn Chaisatit, Chaiyawat Mathavarat, Chantida Praditpol, David Saunders, Kingkan Pidtana, Kirakarn Kirativanich, Kittijarankon Phontham, Mali Ittiverakul, Mark Fukuda, Norman C. Waters, Paphapas Khonhan, Piyaporn Sai-ngam, Sabaithip Sriwichai, and Watcharintorn Fagnark. We appreciate the support of the Thai Ministry of Health teams at Nachaluai, Buntharik, and Ubon Ratchathani. We also appreciate the support of the Office of Disease Prevention and Control 10 and 10.1 (Danai Jaerakul, Chatree Rasribut, Surajit Termwong, Yossunthorn Salabsri, Suwat Dawal, and Supap Silatan), at Vector Borne Disease Control 10.1 Nachaluai (Anichart Santhaweesuk), and at the Buntharik Malaria Clinic (Prasert Surapol and Kreepol Sutawong). Material has been reviewed by the Walter Reed Army Institute of Research. There is no objection to its presentation and/or publication. The opinions or assertions contained herein are the private views of the author and are not to be construed as official or as reflecting true views of the Department of the Army or the Department of Defense. The investigators have adhered to the policies for protection of human subjects as prescribed in AR 70–25.

Author affiliations: [a]Department of Mathematical Sciences, Florida Atlantic University, Boca Raton, FL 33431; [b]Department of Mathematics and Statistics, University of North Carolina, Charlotte, NC 28223; [c]Xilis, Inc., Durham, NC 27713; [d]Department of Biochemistry and Biophysics, University of California, San Francisco, CA 94143; [e]Department of Molecular & Systems Biology, Geisel School of Medicine at Dartmouth, Hanover, NH 03755; [f]Department of Biology, Duke University, Durham, NC 27708; [g]Cymantix, Inc., Durham, NC 27513; [h]Mimetics, LLC., Durham, NC 27707; [i]Sana Biotechnology Inc., Cambridge, MA 02139; [j]Department of Parasitology and Entomology, Faculty of Public Health, Mahidol University, Bangkok 10400, Thailand; [k]US-Armed Forces Research Institute of Medical Sciences, Bangkok 10400, Thailand; [l]Walter Reed National Military Medical Center, Bethesda, MD 20889; [m]U.S. Military HIV Research Program Walter Reed Army Institute of Research, Bethesda, MD 20817; [n]US Naval Medical Research Center-Asia in Singapore, Assigned to Armed Forces Research Institute of Medical Sciences, Bangkok 10400, Thailand; [o]Geometric Data Analytics, Durham, NC 27701; and [p]Department of Medicine Duke University, Durham, NC 27710

1. O. World Health, *World Malaria Report 2021* (World Health Organization, Geneva, 2021).
2. M. Kozlov, Resistance to front-line malaria drugs confirmed in Africa. *Nature* **597**, 604–604 (2021).
3. R. N. Price *et al.*, Global extent of chloroquine-resistant Plasmodium vivax: A systematic review and meta-analysis. *Lancet Infect Dis.* **14**, 982–991 (2014).
4. T. E. Wellems, C. V. Plowe, Chloroquine-resistant malaria. *J. Infect. Dis.* **184**, 770–776 (2001).
5. A. Bykersma, The new zoonotic malaria: Plasmodium cynomolgi. *Trop. Med. Infect. Dis.* **6**, 46 (2021).
6. A. N. Cowell, E. A. Winzeler, The genomic architecture of antimalarial drug resistance. *Brief. Funct. Genomics* **18**, 314–328 (2019).
7. M. M. Ippolito, K. A. Moser, J.-B.B. Kabuya, C. Cunningham, J. J. Juliano, Antimalarial drug resistance and implications for the WHO global technical strategy. *Curr. Epidemiol. Rep.* **8**, 46–62 (2021).
8. F. Rijo-Ferreira *et al.*, The malaria parasite has an intrinsic clock. *Science* **368**, 746–753 (2020).
9. L. M. Smith *et al.*, An intrinsic oscillator drives the blood stage cycle of the malaria parasite *Plasmodium falciparum*. *Science* **368**, 754–759 (2020).
10. P. G. McQueen, F. E. McKenzie, Host control of malaria infections: Constraints on immune and erythropoeitic response kinetics. *PLoS Comput. Biol.* **4**, e1000149 (2008).
11. I. M. Rouzine, F. E. McKenzie, Link between immune response and parasite synchronization in malaria. *Proc. Natl. Acad. Sci. U.S.A.* **100**, 3473–3478 (2003).
12. K. Ikuta, C. Scheiermann, Editorial: Circadian control of immunity. *Front. Immunol.* **11**, 618843 (2020).
13. N. Mideo, S. E. Reece, A. L. Smith, C. J. E. Metcalf, The Cinderella syndrome: why do malaria-infected cells burst at midnight? *Trends Parasitol.* **29**, 10–16 (2013).
14. Y. Yuan, S. Wu, W. Li, W. He, A tissue-specific rhythmic recruitment pattern of leukocyte subsets. *Front. Immunol.* **11**, 102 (2020).
15. I. C. Hirako *et al.*, Daily rhythms of TNFα expression and food intake regulate synchrony of *Plasmodium* stages with the host circadian cycle. *Cell Host. Microbe.* **23**, 796–808.e796 (2018).
16. K. F. Prior *et al.*, Timing of host feeding drives rhythms in parasite replication. *PLoS Pathog.* **14**, e1006900 (2018).
17. A. J. O'Donnell, P. Schneider, H. G. McWatters, S. E. Reece, Fitness costs of disrupting circadian rhythms in malaria parasites. *Proc. Biol. Sci.* **278**, 2429–2436 (2011).
18. S. E. Reece, K. F. Prior, N. Mideo, The life and times of parasites: Rhythms in strategies for within-host survival and between-host transmission. *J. Biol. Rhythms* **32**, 516–533 (2017).
19. R. Zhang, N. F. Lahens, H. I. Ballance, M. E. Hughes, J. B. Hogenesch, A circadian gene expression atlas in mammals: implications for biology and medicine. *Proc. Natl. Acad. Sci. U.S.A.* **111**, 16219–16224 (2014).
20. Z. Bozdech *et al.*, The transcriptome of Plasmodium vivax reveals divergence and diversity of transcriptional regulation in malaria parasites. *Proc. Natl. Acad. Sci. U.S.A.* **105**, 16290–16295 (2008).
21. E. S. Arnardottir *et al.*, Blood-gene expression reveals reduced circadian rhythmicity in individuals resistant to sleep deprivation. *Sleep* **37**, 1589–1600 (2014).
22. C. S. Möller-Levet *et al.*, Effects of insufficient sleep on circadian rhythmicity and expression amplitude of the human blood transcriptome. *Proc. Natl. Acad. Sci. U.S.A.* **110**, E1132–E1141 (2013).
23. T. L. Leise, C. W. Wang, P. J. Gitis, D. K. Welsh, Persistent cell-autonomous circadian oscillations in fibroblasts revealed by six-week single-cell imaging of PER2::LUC bioluminescence. *PLOS One* **7**, e33334 (2012).
24. A. Singer, Angular synchronization by eigenvectors and semidefinite programming. *Appl. Comput. Harmon. Anal.* **30**, 20–36 (2011).
25. S. Jammalamadaka, Y. R. Sarma, "A correlation coefficient for angular variables" in *Statistical Theory and Data Analysis II Proceedings of the Second Pacific Area Statistical Conference*, K. Matusita, Ed. (Elsevier Science Publishers, B.V. North-Holland, Tokyo, 1988), pp. 349–364.
26. F. Hawking, The clock of the malaria parasite. *Sci. Am.* **222**, 123–131 (1970).
27. S. E. Reece, K. F. Prior, Malaria makes the most of mealtimes. *Cell Host. Microbe.* **23**, 695–697 (2018).
28. T. Roenneberg *et al.*, Epidemiology of the human circadian clock. *Sleep Med. Rev.* **11**, 429–438 (2007).
29. D. A. Kalmbach *et al.*, Genetic basis of chronotype in humans: Insights from three landmark GWAS. *Sleep* **40**, zsw048 (2017).
30. M. Sani *et al.*, Daily activity patterns of 2316 men and women from five countries differing in socioeconomic development. *Chronobiol. Int.* **32**, 650–656 (2015).
31. R. Refinetti, Chronotype variability and patterns of light exposure of a large cohort of united states residents. *Yale J. Biol. Med.* **92**, 179–186 (2019).
32. R. Buijs, R. Salgado, E. Sabath, C. Escobar, "Chapter four - peripheral circadian oscillators: Time and food" in *Progress in Molecular Biology and Translational Science*, M. U. Gillette, Ed. (Academic Press, 2013), **vol. 119**, pp. 83–103.
33. M. Gibbs, S. Hampton, L. Morgan, J. Arendt, Adaptation of the circadian rhythm of 6-sulphatoxymelatonin to a shift schedule of seven nights followed by seven days in offshore oil installation workers. *Neurosci. Lett.* **325**, 91–94 (2002).
34. K. F. Prior *et al.*, Host circadian rhythms are disrupted during malaria infection in parasite genotype-specific manners. *Sci. Rep.* **9**, 10905 (2019).
35. U. Abraham *et al.*, Coupling governs entrainment range of circadian clocks. *Mol. Syst. Biol.* **6**, 438–438 (2010).
36. A. E. Granada, H. Herzel, How to achieve fast entrainment? The timescale to synchronization. *PLOS One* **4**, e7057 (2009).
37. S. Bantuchai, H. Imad, W. Nguitragool, Plasmodium vivax gametocytes and transmission. *Parasitol. Int.* **87**, 102497 (2022).
38. S. J. Crowley, C. I. Eastman, Free-running circadian period in adolescents and adults. *J. Sleep Res.* **27**, e12678 (2018).
39. A. J. O'Donnell, K. F. Prior, S. E. Reece, Host circadian clocks do not set the schedule for the within-host replication of malaria parasites. *Proc. R. Soc. B: Biol. Sci.* **287**, 20200347 (2020).
40. A. J. O'Donnell, M. A. Greischar, S. E. Reece, Mistimed malaria parasites re-synchronize with host feeding-fasting rhythms by shortening the duration of intra-erythrocytic development. *Parasite Immunol.* **44**, e12898 (2022).
41. K. F. Prior *et al.*, Synchrony between daily rhythms of malaria parasites and hosts is driven by an essential amino acid. *Wellcome Open Res.* **6**, 186 (2021).
42. D. B. Boivin *et al.*, Circadian clock genes oscillate in human peripheral blood mononuclear cells. *Blood* **102**, 4143–4145 (2003).
43. J. S. O'Neill, A. B. Reddy, Circadian clocks in human red blood cells. *Nature* **469**, 498–503 (2011).
44. A. Dobin *et al.*, STAR: Ultrafast universal RNA-seq aligner. *Bioinformatics* **29**, 15–21 (2013).
45. B. Li, C. N. Dewey, RSEM: Accurate transcript quantification from RNA-Seq data with or without a reference genome. *BMC Bioinformatics* **12**, 323 (2011).
46. F. N. Fritsch, J. Butland, A method for constructing local monotone piecewise cubic interpolants. *SIAM J. Sci. Stat. Computing* **5**, 300–304 (1984).
47. M. E. Hughes, J. B. Hogenesch, K. Kornacker, JTK_CYCLE: An efficient nonparametric algorithm for detecting rhythmic components in genome-scale data sets. *J. Biol. Rhythms* **25**, 372–380 (2010).
48. S. R. Jammalamadaka, A. Sengupta, *Topics in Circular Statistics* (World Scientific, 2001).
49. F. C. Motta, *et al.*, The parasite intraerythrocytic cycle and human circadian cycle are coupled during malaria infection. Gene Expression Omnibus. https://www.ncbi.nlm.nih.gov/geo/query/acc.cgi?acc=GSE209877. Deposited 27 July 2022.
50. F. C. Motta, R. C. Moseley, 2023-Human-Vivax-Coupling (Project ID: 46035634). GitLab. https://gitlab.com/biochron/2023-human-vivax-coupling/. Deposited 15 May 2023.